Published in final edited form as:
J Immunol. 2009 December 15; 183(12): 7877–7889. doi:10.4049/jimmunol.0900834.

Neuronal IκB Kinase β Protects Mice from Autoimmune Encephalomyelitis by Mediating Neuroprotective and Immunosuppressive Effects in the Central Nervous System[1]

Mary Emmanouil[*], **Era Taoufik**[*], **Vivian Tseveleki**[*], **Sotiris-Spyros Vamvakas**[*], **Theodore Tselios**[†], **Michael Karin**[‡], **Hans Lassmann**[§], and **Lesley Probert**[2,*]

[*]Laboratory of Molecular Genetics, Hellenic Pasteur Institute, Athens, Greece

[†]Department of Chemistry, University of Patras, Rio, Greece

[‡]Laboratory of Gene Regulation and Signal Transduction, Department of Pharmacology, University of California San Diego, CA 92093

[§]Center for Brain Research, Medical University of Vienna, Vienna, Austria

Abstract

Some aspects of CNS-directed autoimmunity in multiple sclerosis are modeled in mice by immunization with myelin Ags where tissue damage is driven by myelin-reactive Th1 and Th17 effector lymphocytes. Whether the CNS plays an active role in controlling such autoimmune diseases is unknown. We used mice in which IκB kinase β was deleted from Ca^{2+}/calmodulin-dependent kinase IIα-expressing neurons (nIKKβKO) to investigate the contribution of neuronal NF-κB to the development of myelin oligodendrocyte glycoprotein 35–55-induced experimental autoimmune encephalomyelitis. We show that nIKKβKO mice developed a severe, nonresolving disease with increased axon loss compared with controls and this was associated with significantly reduced CNS production of neuroprotective factors (vascular endothelial growth factor, CSF1-R, and FLIP) and increased production of proinflammatory cytokines (IL-6, TNF, IL-12, IL-17, and CD30L) and chemokines. The isolation of CNS-infiltrating monocytes revealed greater numbers of $CD4^+$ T cells, reduced numbers of $NK1.1^+$ cells, and a selective accumulation of Th1 cells in nIKKβKO CNS from early in the disease. Our results show that neurons play an important role in determining the quality and outcome of CNS immune responses, specifically that neuronal IκB kinase β is required for neuroprotection, suppression of inflammation, limitation of Th1 lymphocyte accumulation, and enhancement of NK cell recruitment in experimental autoimmune encephalomyelitis-affected CNS and stress the importance of neuroprotective strategies for the treatment of multiple sclerosis.

[1]This work was supported in part by the Hellenic Secretariat of Research and Technology, ΠΕΝΕΔ 03ΕΔ827 Grant, by the 6th Framework Program of the European Union, NeuroproMiSe, Grant LSHM-CT-2005-018637, and by a short-term scientific mission grant to V.T. by the European Cooperation in Science and Technology (COST) Action Inflammation in Brain Disease (NEURINFNET) (Grant BM0603).

[2]Address correspondence and reprint requests to Dr. Lesley Probert, Laboratory of Molecular Genetics, Hellenic Pasteur Institute, 11521 Athens, Greece. lesley@pasteur.gr.

Disclosures

The authors have no financial conflict of interest.

Multiple sclerosis (MS)[3] is a chronic inflammatory disease of the CNS in which complex immunopathological mechanisms cause demyelination, neurodegeneration, and progressive neurological disability (1–3). Modern approaches aim to understand the mechanisms underlying inflammatory neurodegeneration and to develop effective neuroprotective therapies for MS (4). Neuroprotection in MS would have a 2-fold benefit: first, because it would slow the neurodegenerative process which starts early in the disease and is probably a secondary consequence of inflammation (3, 5) and, second, because healthy neurons have immune-regulatory effects (6). Thus, although neurons do not normally express MHC class I and II molecules and therefore do not present Ags to T cells (7), they may contribute to the down-regulation of microglia/macrophages by their expression of CD200 (8) or CD22 (9) and interact with T cells to affect their survival (10), bind to them through LFA-1/ICAM-5 interaction (11, 12), and alter their effector phenotype from encephalitogenic T cells to T regulatory cells (13). The mechanisms by which neurons and axons are damaged in MS and its best-studied animal model experimental autoimmune encephalomyelitis (EAE) are not yet known, but the MS-associated immune mediator TNF is known to exert strong neuroprotective effects in other disease models of excitotoxic and ischemic injury through the induction of NF-κB activity in neurons (14–17) and the maintenance of several integrated neuroprotective pathways (18). We hypothesized that NF-κB activity might be important for protecting neurons during the development of EAE and thereby also modulate the encephalitogenic response within the CNS tissues.

The transcription factor NF-κB mediates many of the effects of inflammatory stimuli through induction of genes encoding for cytokines, chemokines, adhesion molecules, growth factors, and antiapoptotic molecules (19, 20). In addition, NF-κB controls transcription of HIF-1α, the oxygen-regulated subunit of the hypoxia-inducible transcription factor HIF-1 and the induction of HIF-1α target genes (21). NF-κB activation is controlled by IκB kinases, mainly IKKβ, which phosphorylate and mediate the degradation of IκB, thereby allowing NF-κB to translocate to the nucleus to bind to κB sequences on DNA (22). Conditional gene targeting of vital NF-κB components, such as IKKβ, in selected cell lineages of mice has allowed the study of cell-specific NF-κB function in adult mice under physiological and pathological conditions. In the normal CNS, NF-κB is constitutively active in neurons and is further activated by basal synaptic input and glutamate in a Ca^{2+}-dependent manner in hippocampal neurons (23). Neuronal NF-κB regulates spatial memory formation and synaptic transmission and plasticity in mice (23–25). In CNS pathology, however, the role of NF-κB is much less clear. NF-κB becomes activated in most cell types, particularly neurons, astrocytes, and microglia, and both neurotoxic (26) and neuroprotective (27–29) effects have been described. The mechanisms that underlie such diverse effects of NF-κB and one of its main activating ligands TNF in the CNS are not yet fully understood, but are likely to reflect complexities in the cellular basis of their action and the different mechanisms of injury. The deletion of IKKβ from Ca^{2+}/calmodulin-dependent kinase IIα

[3]Abbreviations used in this paper: MS, multiple sclerosis; CamkII, Ca^{2+}/calmodulin-dependent kinase IIα; EAE, experimental autoimmune encephalomyelitis; IKKβ, IκB kinase β; *lacZ*, β-galactosidase gene; MOG, myelin oligodendrocyte glycoprotein; VEGF, vascular endothelial growth factor; CamkIICre, CamkII promoter-derived Cre recombinase; WT, wild type; LN, lymph node; NeuN, neuronal nuclei; GD, glucose deprivation; LDH, lactate dehydrogenase; hTNF, human TNF.

(CamkII)- expressing neurons or neurons/astrocytes (30) and neuronal inactivation of NF-κB (31) in mice significantly reduced lesion volume following experimental cerebral ischemia, supporting a deleterious effect of neuronal NF-κB in acute ischemic injury. The deletion of IKKβ from astrocytes or microglia enhanced astrogliosis and reduced vascular endothelial growth factor (VEGF) expression in a hypoxia model (21), indicating protective effects of glial IKKβ following hypoxia. On the other hand, the deletion of IKKγ/NEMO or IKKβ from neurons/astrocytes (32) or the inactivation of NF-κB in astrocytes (33) resulted in significant amelioration of EAE showing that NF-κB-mediated astrocyte activation has deleterious effects in this model of chronic CNS inflammation (32, 34). The role of neuronal NF-κB activity in EAE remains unknown.

In this study, we used mice in which IKKβ was selectively deleted in CamkII-expressing neurons in the brain and spinal cord to clarify the role of neuronal NF-κB during the development of EAE. Furthermore, we investigated the effect of neuronal IKKβ upon the regulation of CNS immune reactivity and infiltration by specific populations of immune cells. Our data show that NF-κB activation through IKKβ is critical for neuron-mediated immunoregulation during the development of autoimmune demyelination, where it is important for neuroprotection and limitation of axon loss, for suppression of CNS inflammation and prevention of Th1 effector cell accumulation, and for enhancing the recruitment of NK cells in the CNS.

Materials and Methods

Generation of nIKKβKO mice

Mice containing a conditional IKKβ allele in which exon 3 of the *Ikbkb* gene, encoding the IKKβ activation loop, is flanked by *loxP* sites (IKKβ$^{F/F}$) have been previously described (35, 36). Mice with a selective deletion of IKKβ in CNS neurons (nIKKβKO) were generated by crossing IKKβ$^{F/F}$ mice with mice that express a neuronal CamkII promoter-driven Cre recombinase (CamkIICre) (37). We used a ROSA26 Cre reporter mouse strain, which expresses *lacZ* following Cre recombination (38) (ROSA26) to monitor the cell specificity of Cre expression in CamkIICre mice. All mice used in this study were backcrossed into the C57BL/6 genetic background for at least seven generations. Mice were kept under specific pathogen-free conditions in the experimental animal unit of the Hellenic Pasteur Institute. All animal procedures were approved by national authorities and conformed to European Community guidelines.

Synthesis and purification of $MOG_{35–55}$

$MOG_{35–55}$ was synthesized in solid phase by F-moc/tBu methodology using the 2-chlorotrityl chloride resin (0.6–1.0 mmol Cl^-/g) and the appropriate N^{α}-F-moc-protected amino acids (39, 40). The final product was further purified using semipreparative RP-HPLC. The purity of peptide was determined using analytical RP-HPLC, and its identification was achieved by electron spray ionization-mass spectrometry.

EAE induction and evaluation

Experiments were performed in female C57BL/6 wild-type (WT), nIKKβKO, and IKK$\beta^{F/F}$ littermate control mice of 8–10 wk of age. EAE was induced by s.c. tail base injection of 30 μg of $MOG_{35–55}$ dissolved in 100 μl of saline and emulsified in 100 μl of CFA (Sigma-Aldrich) supplemented with 300 μg of H37Ra *Mycobacterium tuberculosis* (Difco). Mice also received an i.p. injection of 200 ng of pertussis toxin (Sigma-Aldrich) on days 0 and 2. Mice were assessed daily for clinical signs as previously described (41). Moribund animals were sacrificed. Mice were allowed free access to food and water throughout the experiment.

T cell priming and proliferation assay

T cells were primed in vivo by s.c. injection of control and nIKKβKO mice with 30 μg of $MOG_{35–55}$ peptide dissolved in 100 μl of saline and emulsified in 100 μl of CFA (Sigma-Aldrich). Draining lymph nodes (LN) and spleens were removed 9 days after immunization and isolated cells were cultured as described previously (41). Results are expressed as the stimulation index (ratio between radioactivity counts of cells cultured in the presence of Ag and cells cultured with medium alone).

Extraction and characterization of CNS-infiltrating cells

Draining LN cells, splenocytes, and spinal cord mononuclear cells were isolated from mice at the peak and chronic phase of EAE. Mononuclear cells from the spinal cords were isolated by Percoll gradient centrifugation as previously described (42). For detection of cell surface markers, cells were washed and fixed in 2% paraformaldehyde solution in PBS for 15 min at room temperature. For intracellular staining, after isolation cells were restimulated with 10 ng/ml PMA, 1 μg/ml ionomycin in the presence of 5 μg/ml brefeldin A (Sigma-Aldrich) for 3 h, and subsequently fixed in 2% paraformaldehyde solution in PBS for 15 min at room temperature. For the detection of cell surface markers, cells were stained with fluorochrome-labeled Abs (anti-CD8a, clone Ly-2; anti-CD45R/B220, clone RA3-6B2; anti-NK1.1, clone PK136; anti-CD11b/Mac1, clone M1/70; BD Biosciences). For the detection of CD4 and CD25 cell surface markers and intracellular cytokines by FACS analysis, cells were permeabilized with 0.5% w/v saponin and stained with fluorochrome-labeled Abs (anti-CD4, clone L3T4; anti-CD25/IL-2Ra, clone 7D4; anti-FoxP3, clone FJK-16s; anti-IL-17, clone TC11-18H10; anti-IFN-γ, clone XMG1.2; BD Biosciences). Data acquisition was done with a FACSCalibur cytometer and CellQuest software (BD Biosciences).

Cytokine measurements

The murine Th1/Th2 cytokine cytometric bead array kit (BD Biosciences) was used to measure cytokine levels in lymphocyte cell culture supernatants from nIKKβKO and control mice according to the manufacturer's instructions. The cytokines measured were IL-2, IL-4, IL-5, IFN-γ, and TNF-α. The sensitivity of the assays for different cytokines was as follows: IL-2, IL-4, and IL-5 = 5.0 pg/ml, IFN-γ = 2.5 pg/ml, and TNF-α = 6.3 pg/ml. Data acquisition was done with a FACSCalibur cytometer and CellQuest software (BD Biosciences) and data analysis with CBA analysis software (BD Biosciences).

Histopathological analysis

Mice were transcardially perfused with ice-cold 4% paraformaldehyde in PBS under deep anesthesia. CNS tissues were postfixed in the same fixative overnight at 4°C and processed for standard histopathological and immunohistochemical analyses. Inflammation was visualized by H&E, demyelination by Luxol fast blue, and axonal damage by Bielchowsky silver staining. Immunohistochemistry was performed on paraffin sections as previously described (43) to evaluate CNS infiltration by T cells and macrophages. Ag retrieval in paraffin sections was done in a household food steamer in citrate buffer (pH 5) for 1 h. Primary Abs used were rat anti-human CD3 (1/400; Serotec), anti-Mac3 (1/100; BD Biosciences), and rabbit anti-$FLIP_{S/L}$ (1/1000; Santa Cruz Biotechnology). For immunofluorescence staining, cryostat sections (10 μm) were incubated with rabbit anti-neuronal nuclei (NeuN) (1/100; Chemicon International), mouse anti-IKKκ (1/100; Cell Signaling), and mouse anti-$FLIP_{S/L}$ (1/100; Santa Cruz Biotechnology) primary Abs, separately or together, and visualized by Alexa Fluor 568 anti-rabbit IgG (green) and Alexa Fluor 488 anti-mouse IgG (red) secondary Abs (Molecular Probes), respectively, using a confocal microscope.

lacZ staining

Mice containing the β-galactosidase (*lacZ*) reporter allele (ROSA26) were transcardially perfused with ice-cold 4% paraformaldehyde in PBS under deep anesthesia and CNS tissues were postfixed in the same fixative for 2 h at 4°C. Brain and spinal cord 25-μm cryostat sections were processed for *lacZ* staining using 5-bromo-4-chloro-3-indolyl β-D-galactopyranoside (X-Gal) (Promega) as substrate according to manufacturer's instructions.

Primary cultures of neocortical neurons and experimental treatments

Dissociated neocortical cell cultures were prepared from E15 control and nIKKβKO mice and treated as described previously (16, 44). Glucose deprivation (GD) of neuron cultures was performed as previously described (16). Human recombinant TNF (hTNF) (R&D Systems) was added to cultures 24 h before the onset and during GD. Measurement of lactate dehydrogenase (LDH) released from damaged neurons into the culture medium was performed as described previously (45) and culture medium from untreated neurons was used for normalization.

EMSA

EMSAs were performed using 30 μg of protein extracts from primary cortical neurons treated with 10 and 100 ng/ml hTNF for 20 min (protein extracts were prepared as described above) from representative control and nIKKβKO mice. Proteins were incubated with a NF-κB double-stranded oligonucleotide containing the consensus binding site of the κB enhancer (AGT TGA GGG GAC TTT CCC AGG C) that was end-labeled with [γ-^{32}P]ATP using T4 kinase (Promega) in the following buffer: 10 μg/ml BSA, 20 mM HEPES (pH 7.5), 1 mM EDTA, 1% Nonidet P-40, 5% glycerol, 5 mM DTT, and 0.15 mg/ml poly(dI:dC). DNA protein complexes were resolved on 4% native polyacrylamide gels. To determine specificity of the complexes, competition experiments were performed by incubating selected protein extracts with an excess of unlabeled consensus.

Western blot analysis

Total protein extracts from selected subregions of the CNS and other tissues (spleen, thymus, LN, liver, and gonads) of nIKKβKO and control mice were prepared as previously described (16). Thirty micrograms of total protein extracts were resolved on NuPAGE Novex Bis-Tris Gels (Invitrogen) and transferred onto nitrocellulose membranes (Schleicher & Schuell Microscience). Blots were probed with Abs against IKKβ (1/200; Upstate Biotechnology), phospho-IκBα (1/500; Cell Signaling), and phospho-p65 (1/250; Cell Signaling). The secondary Abs used were HRP-conjugated anti-mouse and anti-rabbit IgG (1/2000 up to 1/5000; Jackson ImmunoResearch Laboratories). Ab binding was detected using the ECL Plus detection system (Amersham Pharmacia). To normalize for protein content, we stripped and reprobed membranes with anti-β-tubulin Ab (1/1000; BD Pharmingen).

Ab array for mouse cytokine expression

Two different Ab array platforms carrying immobilized capture Abs were used, one for 65 different soluble signaling factors and cytokines (Chemi- Array Mouse Cytokine Ab Array III; Chemicon International) (see Fig. 4) and the other for 18 factors (TranSignal Mouse Cytokine Ab Array 1.0; Panomics) (data not shown) according to the manufacturer's instructions. Membranes were incubated with 200–400 μg of total protein lysates isolated from the spinal cord of control (n = 4) and nIKKβKO (n = 4) mice at day 22 after EAE induction. Signals were detected using chemiluminescence detection reagent with multiple exposures to Kodak X-Omat film. Signal intensity was quantified by densitometry using Image Quant 5.2 (Molecular Dynamics Storm Scanner 600). Sample spots were normalized against positive control spots on each individual membrane. Normalized data were used to show fold changes in cytokine expression of nIKKβKO compared with control lysates. The mean fold change ± SEM from two independent experiments for the first array platform are presented (see Fig. 4).

Total RNA isolation, semiquantitative and quantitative RT-PCR

Total RNA was extracted with TRIzol (Invitrogen) according to the manufacturer's instructions. For semiquantitative RT-PCR, DNase-treated (Promega) RNA was reverse transcribed with M-MLV Reverse Transcriptase (Promega) and random hexamers (Roche). Primers were used for the detection of FLIP (forward, 5′-GAA GAG TGT CTT GAT GAA GA-3′ and reverse, 5′-GAA AAG CTG GAT ATG ATA GC-3′), VEGF (forward, 5′-GCG GGC TGC CTC GCA GTC-3′ and reverse, 5′-TCA CCG CCT TGG CTT GTC AC-3′), and CSF-1R (forward, 5′-GAC CTG CTC CAC TTC TCC AG-3′ and reverse, 5′-GGG TTC AGA CCA AGC GAG AAG- 3′). Mouse β-actin was amplified as a loading control. Densitometric analysis was performed using Image Quant 5.2 (Molecular Dynamics Storm Scanner 600) and relative band intensities were determined. Quantitative RT-PCR for TNF and CXCL16 was performed using a QuantiFast SYBR green RT-PCR kit (Qiagen) according to the manufacturer's instructions. QuantiTect Primer Assays were used for TNF, CXCL16, and β-glucuronidase (Qiagen). All reactions were performed using the LightCycler System (Roche). At the end of each PCR run, melting curve analysis was also performed to verify the integrity and homogeneity of PCR products. Gene expression levels

were calculated using already created standard curves for each gene. These standard curves were created by plotting threshold cycle values vs the logarithm of serial diluted RNA concentrations. Least-squares methods were used for the determination of *A* and *B* values in the equation threshold cycle = A*log(C_{RNA}) + B. The coefficient of determination (R^2) was >0.99. Values were normalized using the respective *β*-glucuronidase values.

Statistics

All statistical analyses were performed with SigmaStat 2.0 for Windows. All data are given as mean ± SEM. For comparisons of neuron viability as measured by LDH release (see Fig. 2, *C* and *D*), one-way ANOVA with Bonferroni correction was performed. To determine significant differences between clinical scores of control and nIKK*β*KO mice at different time points after immunization (see Fig. 3*A*), the Mann-Whitney rank sum test was performed. Student's *t* test was used to compare the inflammatory infiltrates (see Fig. 3*G*), FLIP expression in spinal cord neurons (see Fig. 5*C*) and lymphocyte populations analyzed by FACS (see Fig. 6, *C* and *D*) between control and nIKK*β*KO mice after immunization. For semiquantitative RT-PCR analyses, the Mann-Whitney rank sum test or one-way ANOVA followed by the Bonferroni *t* test for pairwise comparisons was performed (see Figs. 4, *D* and *E*, and 5*D*). For quantitative RT-PCR analyses (see Fig. 4, *B* and *C*), differential expression between control and nIKK*β*KO samples at each time point was evaluated using the Mann- Whitney rank sum test. Differences between the normalized cytokine levels from two experiments for each Ab array platform were determined using the Mann-Whitney rank sum test (see Fig. 4*A*). Values of $p < 0.05$ were considered statistically significant.

Results

Conditional deletion of IKKβ in CNS neurons

For the conditional deletion of *loxP*-flanked genes in CNS neurons, we used transgenic mice expressing Cre recombinase under the control of the CamkII promoter (CamkIICre) as previously described (37). The selective deletion of IKK*β* from CamkII-expressing neurons was relevant for this study given the reported involvement of NF-*κ*B in Ca^{2+}-regulated, CamkII-dependent signaling in neurons (23) and the importance of axonal Ca^{2+} channels in EAE and MS (46, 47). CamkIICre mice have already been extensively characterized and used (29, 48) and we further characterized the pattern of Cre-mediated gene deletion in our system by crossing CamkIICre mice with the ROSA26 reporter strain which carries a *loxP*-flanked neo "stop" cassette within the coding sequence of *β*-galactosidase gene (38). *LacZ* staining of CamkIICreROSA tissue sections revealed the location of Cre-mediated *loxP* recombination in neurons widely distributed within the forebrain, including cortex, hippocampus, and striatum (Fig. 1A, *left panel*) and Purkinje cells of the cerebellum (Fig. 1A, *right panel*) as previously described (37), as well as in the spinal cord in nerve endings in lamina I and neuron cell bodies located in the outer laminas II–III of the dorsal horn, lamina X around the central canal, and sparse neurons in the ventral horn (Fig. 1B, *right panel*). To achieve *Ikbkb* gene deletion in CNS neuronal populations, we crossed IKK$\beta^{F/F}$ mice (35, 36) with CamkIICre-transgenic mice (nIKK*β*K; Fig. 1*C*). nIKK*β*K mice developed and reproduced normally and had no obvious abnormalities.

Western blot analysis of protein extracts from mouse tissues demonstrated efficient CNS-specific depletion of IKKβ in nIKKβKO mice compared with control mice (Fig. 1*D*). Specifically, there was complete IKKβ depletion in cortex and hippocampus and a marked reduction in striatum, cerebellum (Fig. 1*E*), and spinal cord (Fig. 1*D*). No differences in IKKβ expression were detected in non-CNS tissues, including thymus, spleen, and LN between nIKKβKO and control mice (Fig. 1*D*). The neuronal basis of IKKβ depletion was further verified using extracts from enriched (estimated >95%) cultures of primary cortical neurons isolated from nIKKβKO mice that showed a high level of recombination (Fig. 1*F*). Because the expression of CamkIICre within neuronal populations of the spinal cord has not been well characterized, we also directly compared the distribution of IKKβ-immunoreactive cells within spinal cord sections from control and nIKKβKO mice by immunohistochemistry. IKKβ was expressed by cells distributed throughout the spinal cord in both mouse strains; therefore, we compared the colocalization of IKKβ with NeuN in spinal cord neurons to evaluate the extent of deletion from neurons in nIKKβKO mice. In control cord, IKKβ-positive neurons were localized throughout the gray matter including laminas II–III of the dorsal horn, lamina X around the central canal (Fig. 1*G*), and numerous neurons in the ventral horn. In addition, large numbers of spinal cord axons originating in proximal brain and spinal cord neurons should also contain IKKβ. In contrast, IKKβ-positive neurons were markedly reduced in cord from nIKKβKO mice, particularly in cells localized in the dorsal horn and around the central canal (Fig. 1*G*).

To verify that the canonical NF-κB pathway is also functionally inactive in nIKKβKO neurons, we treated neurons from both strains with human TNF (hTNF) and measured the levels of NF-κB activity by EMSA. In control neurons, constitutive NF-κB activity was detectable corresponding to p50/p65 heterodimers (upper band) and p50/p50 homodimers (lower band) and was induced by TNF treatment (Fig. 2*A*). In contrast, p50/p50 activity was low and p50/p65 activity was completely absent in nIKKβKO neurons and were not altered by TNF treatment (Fig. 2*A*). Constitutive levels of pIκBα were detected in neurons from both strains and were further induced after TNF treatment in a dose-dependent manner in control, but not nIKKβKO, neurons (Fig. 2*B*). Constitutive levels of phospho-p65 were also detectable in control neurons and were further induced by TNF treatment in a dose-dependent manner (Fig. 2*B*). In contrast, phospho-p65 was not detectable in nIKKβKO neurons (Fig. 2*B*). We further investigated the contribution of IKKβ to neuron survival in in vitro models of neurotoxicity. hTNF administration induced dose-dependent cell death in nIKKβKO neurons (Fig. 2*C*), a finding consistent with the known role of NF-κB in mediating cytoprotection against TNF. Furthermore, hTNF pretreatment, that is known to protect primary cortical neurons against excitotoxic and ischemic injury (14, 16), failed to induce neuroprotection in nIKKβKO neurons after GD (Fig. 2*D*).

Neuronal IKKβ deficiency results in severe nonresolving neurological defects in the chronic phase of EAE

To study the function of IKKβ in neurons during a chronic demyelinating and neurodegenerative disease, we used the $MOG_{35–55}$-EAE model for MS, which is characterized by a chronic nonrelapsing clinical course in C57BL/6 mice and shows neuronal damage and forebrain involvement (49). We immunized C57BL/6 WT, IKK$\beta^{F/F}$

littermate controls, and nIKKβKO mice with $MOG_{35–55}$ and measured their clinical symptoms daily. The IKK$\beta^{F/F}$ controls and WT mice both showed typical clinical symptoms of $MOG_{35–55}$-EAE with an acute initial phase followed by gradual disease resolution (Fig. 3*A* and Table I). In contrast, mice lacking neuronal IKKβ showed significantly enhanced clinical symptoms (Fig. 3*A* and Table I). In a representative experiment from three (experiment 3), nIKKβKO mice had the same disease onset as IKK$\beta^{F/F}$ controls but developed a significantly more severe, nonremitting form of disease with significantly increased clinical score until the last time point tested ($p < 0.05$, days 19–42 after immunization inclusive; Fig. 3A). A number of animals in the nIKKβKO group became moribund during the experiment and were euthanized on days 26 and 34 (Table I). These mice were given a clinical score of 5 for the remaining days of the experiment.

Sustained severe neuropathology in neuronal IKKβ-deficient mice

To investigate whether the enhanced neurological defect in nIKKβKO mice was associated with differences in neuropathology, we examined spinal cord sections from nIKKβKO and control mice taken at different time points: peak of disease (day 17) and early (day 22) and late (days 34 and 42) chronic phase. At day 17, both nIKKβKO and control mice showed severe infiltration of the meninges and spinal cord parenchyma by immune cells as visualized by H&E staining and anti-Mac3 immunohistochemistry (Fig. 3, *B* and *E*). Demyelination, shown by Luxol fast blue staining (Fig. 3*C*), and axonal damage, shown by Bielschowsky silver staining (Fig. 3*D*), were observed in both groups of mice to a similar extent. At days 22 and 42, immune cell infiltration appeared less severe than at day 17 in control, but not nIKKβKO mice (Fig. 3, B, E, and F). At days 22 and 42, demyelination appeared more severe than at day 17 in nIKKβKO, but not control mice (Fig. 3*C*). Quantitative analysis of neuropathological changes did not reveal differences in inflammatory cell infiltration in spinal cords from the two mouse strains (Fig. 3*G*) but did reveal significantly increased axon loss in nIKKβKO spinal cords compared with those from control mice at day 34 (Fig. 3*H*). Axonal pathology was further evaluated by immunohistochemistry using an Ab to amyloid precursor protein. Axonal amyloid precursor protein accumulation was evident on day 17 and axon damage was exacerbated by day 22 in both groups of mice. nIKKβKO mice showed more frequent and larger lesions than control mice by day 42 (data not shown).

Neuronal IKKβ suppresses the production of inflammatory mediators and enhances the expression of neuroprotective factors in the spinal cord during EAE

Comparison of the production of immune mediators in spinal cord protein extracts taken at day 22 of EAE using an Ab array panel showed that a number of key lymphokines, chemokines, and other neuroactive molecules were differentially regulated in nIKKβKO mice compared with control mice. Specifically, Th1 (IL-12 p40/p70, IL-12p40, TNF), Th17 (IL-17), and proinflammatory (IL-6, TNF) cytokines, proinflammatory chemokines (KC/CXCL1, MCP-1/CCL2, RANTES/CCL5, CTACK/CCL27, TECK/CCL25, CXCL16/scavenger receptor, MCP-5/CCL12, MIP-1α/CCL3, TARC/CCL17, TCA-3/CCL1), and several other mediators (tissue inhibitor of metalloproteinase 1, leptin receptor, TNFRI, TNFRII, thrombopoietin) were significantly up-regulated in the spinal cord of mice with neuronal deletion of IKKβ at day 22 of EAE (Fig. 4*A*). Only a few proteins showed

significant down-regulation and these included IL-10, an immunomodulatory cytokine, and VEGF, a neuroprotective factor (Fig. 4*A*). A large number of proteins was not significantly regulated in the nIKKβKO EAE spinal cord (supplemental Table SI).[4] The differential expression of several targets was further validated at the mRNA level by semiquantitative and quantitative RT-PCR in independent samples. The expression of CXCL16 and TNF mRNA was significantly increased in nIKKβKO spinal cord at day 17 of EAE compared with control as determined by quantitative RT-PCR (Fig. 4, *B* and *C*). Also, mRNA expression of the neuroprotective factors, CSF-1R (Fig. 4*D*), VEGF (Fig. 4*E*), and FLIP (Fig. 5*D*) was significantly decreased by day 22.

To investigate the effect of neuronal IKKβ deletion upon the cellular localization of FLIP, a NF-κB-inducible neuroprotective protein (16, 50), during EAE, we performed immunocytochemistry on sections of spinal cord and brain taken at day 22 of EAE. In control tissues, FLIP immunoreactivity was localized mainly in neurons in the outer laminas of the dorsal horn (Fig. 5A, i and ii) and large neurons of the ventral horn (Fig. 5*Aiii*) of the spinal cord, as well as Purkinje cells (data not shown), hippocampal neurons (Fig. 5Aiv), and large cortical neurons (Fig. 5*Av*) of the brain. $FLIP_{S/L}$ immunoreactivity colocalized with the neuronal marker NeuN in a large proportion of cells, confirming the neuronal localization of FLIP and that FLIP is mainly expressed by neurons in the gray matter of the dorsal and ventral horns of the spinal cord (Fig. 5*B*). FLIP immunoreactivity was markedly reduced in the spinal cord of nIKKβKO mice compared with control mice at day 22 of EAE (Fig. 5A, i–v) and this was correlated with a significant reduction in the number of FLIP-immunoreactive spinal cord neurons (Fig. 5*C*) and levels of FLIP mRNA in spinal cord extracts (Fig. 5*D*).

Th1 effector T cell enrichment and NK cell deficit in the CNS of neuronal IKKβ-deficient EAE mice

The expression of IKKβ in thymus, LN, and spleen of nIKKβKO mice was comparable to that in control mice (Fig. 1*D*). To analyze T cell responses to Ag priming, mice were immunized with $MOG_{35–55}$ and cells were isolated from draining LN and spleens 9 days later and restimulated in vitro with $MOG_{35–55}$ peptide. Cells derived from nIKKβKO and control mice showed equivalent recall responses to $MOG_{35–55}$ peptide (Fig. 6, *A* and *B*). Also, measurement of cytokine secretion did not reveal an increase in the production of IFN-γ and TNF-α by the nIKKβKO cells (data not shown). These results show that the observed exacerbation of clinical disease in nIKKβKO mice is unlikely to be due to alterations in T cell priming to $MOG_{35–55}$.

To investigate whether the increased levels of proinflammatory cytokines measured in spinal cord extracts from nIKKβKO EAE mice were reflected by differences in CNS-infiltrating immune cell populations, we isolated mononuclear cells from the spinal cords of mice with active EAE at the peak (clinical score 3.5–4 in both strains) and chronic phase time points and measured the proportions of the major immune cell populations known to be associated with EAE, as well of cytokine-producing cells compared with those in splenocytes and

[4] The online version of this article contains supplemental material.

draining LN cells isolated from the same animals. Equivalent numbers of mononuclear cells were isolated from EAE spinal cords from the two mouse strains. No differences in the proportions of spinal cord $CD8^+$ or $CD25^+FoxP3^+$ T cells, $B220^+$ B cells, or $CD11b^+$ macrophages were detected between the two strains at either time point (Fig. 6, *C* and *D*). A significant increase in the proportion of $CD4^+$ T cells and a significant decrease in the proportion of $NK1.1^+$ cells were observed in the spinal cord compared with controls at both time points (Fig. 6*C*). Furthermore, intracellular staining of cytokines within the pool of CNS-infiltrating monocytes at the peak and chronic phase time points revealed a significant increase in the proportion of $CD4^+$ IFN-γ^+ cells in the nIKKβKO compared with control spinal cord (Fig. 6, *D* and *E*), but not $CD4^+$IL-17^+ cells (Fig. 6*D*). In contrast, the pools of $CD4^+$IFN-γ^- and $CD4^+$IL-17^- cells were unaltered. The CNS specificity of the enhanced Th1 cell representation in nIKKβKO mice was confirmed by the finding that splenic and LN $CD4^+$IFN-γ^+ and $CD4^+$IL-17^+ cells were equivalent in nIKKβKO and control mice with EAE (Fig. 6*D*). These results show that there is a selective enrichment of $CD4^+$IFN-γ^+ CNS-infiltrating T cells and a decrease in $NK1.1^+$ cells in the nIKKβKO spinal cord during the development of EAE and suggest that one of the protective effects of neuronal IKKβ during the development of EAE is to selectively limit the accumulation of proencephalitogenic Th1 cells and enhance the accumulation of $NK1.1^+$ cells within the CNS microenvironment.

Discussion

The role of NF-κB in CNS neurons and its contribution to neurodegeneration during disease is important to define, particularly in view of current efforts to develop more selective blocking reagents for NF-κB and one of its major inducers, TNF, for the treatment of a variety of inflammatory conditions and cancer (51). In this study, we addressed the specific contribution of IKKβ in CamkII-expressing neurons to the development of EAE, an autoimmune model for MS that is characterized by CNS inflammation, demyelination, and early axonal damage. We show that neuronal IKKβ does not affect the initiation of EAE but plays important roles in inducing the production of neuroprotective molecules, in modulating the CNS inflammatory response, and in regulating the accumulation of specific immune cell populations in the spinal cord after the induction of disease with the result of protecting mice against the development of severe neurologic impairment. Our findings demonstrate that neurons play an important immunoregulatory role during the development of autoimmune demyelination and identify IKKβ as a critical neuronal molecule that links neuroprotection with neuron-mediated suppression of CNS inflammation.

One mechanism by which neuronal NF-κB activation through IKKβ protects mice during EAE is by mediating neuroprotection. The neuroprotective properties of NF-κB have been well described in various models of neuron injury. Thus, neuronal NF-κB activity is necessary for TNF-induced neuroprotection against excitotoxic and ischemic injury, is central to ischemic tolerance, and protects mice against secondary lesion expansion following cerebral ischemia (52, 53). In the present study, nIKKβKO mice showed significantly enhanced spinal cord axon loss during EAE and this was associated with significant reduction in the expression of known neuroprotective factors, VEGF, CSF-1R, and FLIP in cord extracts. VEGF is a NF-κB-inducible gene (54) and is also responsive to HIF-1 which is NF-κB dependent (21). It is produced by neurons and astrocytes and has

neurotrophic and neuroprotective effects in isolated neurons, mediates tolerance induction, neuroprotection, and enhances the survival of new neurons in experimental ischemia in mice (55–57). It also protects motor neurons in a model for amytropic lateral sclerosis (58, 59). CSF-1R is constitutively expressed by CNS neurons and further up-regulated following ischemic injury (60) and in EAE and MS brain (61). Its ligand CSF-1 (murine M-CSF) protects neurons and suppresses microglial activation during development and following ischemia (62–64). The antiapoptotic protein FLIP is another NF-κB-inducible protein (50) expressed by brain neurons that shows neuroprotective properties in experimental ischemia (16). Importantly, the absence of IKKβ from CNS neurons did not significantly affect the basal levels of mRNA expression of these three neuroprotective proteins in the spinal cord before EAE. Following EAE induction, however, nIKKβKO mice were unable to maintain or up-regulate the expression of mRNAs for VEGF, CSF-1R, or FLIP in the spinal cord or to maintain FLIP immunoreactivity in spinal cord neurons, indicating that neuronally located NF-κB plays a major role in inducing the expression of VEGF, CSF-1R, and FLIP in spinal cord tissues during EAE.

The immune regulatory properties of neurons in the normal CNS have been addressed in several earlier studies (6, 65). Neurons constitutively express the immunosuppressive cytokine TGF-β (13, 66), the T cell costimulatory ligands B7.1 and B7.2 (13), and two negative regulators of the macrophage lineage, CD200 and CD22 (8, 9). Indeed, CD200-deficient mice show spontaneously enhanced microglial activation and develop significantly advanced EAE compared with control mice (8). Neuronal electrical activity is also important for counterregulating immune reactivity in surrounding astrocytes and microglia because IFN-γ can induce MHC class II molecule expression and therefore Agpresenting properties in these cells in brain slices, only in the presence of a sodium channel antagonist, presynaptic calcium channel blockers, or glutamate receptor antagonists (67, 68). However, it has been unclear whether neurons maintain their immune regulatory properties during CNS inflammation and, if so, which are the mechanisms involved. Previous studies have shown that functionally compromised neurons become sensitive to IFN-γ-induced MHC class I expression and therefore may directly interact with $CD8^+$ T cells (7) and that stressed neurons can induce apoptosis in activated microglia via Sema3A/Neuropilin 1 interaction (69). Major findings of the present study are that neurons have a significant anti-inflammatory effect in the CNS microenvironment during the development of autoimmune demyelination and that neuronal NF-κB activity is identified as a critical mediator of this effect. Neuronal deficiency of IKKβ did not alter the basal expression of the inflammatory markers measured here and nIKKβKO mice were phenotypically normal, suggesting that neuronal NF-κB activity is not necessary for the maintenance of immune quiescence in the CNS under normal conditions. Following the induction of EAE, however, neuronal NF-κB activity was essential for counterregulating the production of immune mediators that have been positively associated with EAE and MS. These included chemokines involved in the attraction and recruitment of monocytes and activated lymphocytes into tissues (MCP-1/CCL2, RANTES/CCL5, TECK/CCL25, CXCL16) (70), proinflammatory cytokines (IL-6, TNF, TNFRI), as well as cytokines involved in Th1 (IL-12 p70) and Th17 (IL-17, CXCL1) (71) responses. Of note, production of the immunosuppressive cytokine IL-10 was reduced in the nIKKβKO EAE spinal cord. We also showed that neuronal NF-κB activity is

necessary for enhancing the accumulation of NK1.1$^+$ cells and for limiting the accumulation of CD4$^+$IFN-γ^+, but not CD4$^+$IL-17$^+$, T cells in spinal cord tissues from early in the disease. CD4$^+$IFN-γ^+ Th1-polarized myelin-reactive T cells are capable of triggering EAE by adoptive transfer into naive recipient mice (72) and NK1.1$^+$ cells, including the NK T cell population, have disease-protective effects (73). It is possible that both of the immune cell changes observed in nIKKβKO EAE spinal cord promote disease severity in these mice. Our results show that a major role of neuronal IKKβ is to maintain the integrity of neurons and thereby suppress the proinflammatory environment of the CNS tissue during EAE. One hypothesis would be that TNF, which is rapidly and highly up-regulated by activated microglia/macrophages and T cells in the vicinity of neurons during EAE, could serve as an activating ligand for neuronal TNFRI and TNFRII, both of which mediate neuroprotection through the induction of NF-κB activity (14, 15, 74, 75). Our present findings support the contention that under conditions of inflammation, a neuronal TNF-TNFRI-NF-κB pathway would be activated which would mediate neuroprotection and feedback to negatively regulate glial immunoreactivity.

It will be important to define the molecular mechanism by which neuronal IKKβ suppresses brain inflammation and the accumulation of proinflammatory T cells, as well as enhances the accumulation of NK1.1$^+$ cells, in the CNS in EAE as new therapeutic targets. Neurons are known to suppress the reactivity of neighboring cells in the normal CNS and it is likely that they do the same under disease conditions. Alterations in cytokine and chemokine production by these cells could clearly shape the quality and quantity of CNS-infiltrating monocyte populations, a mechanism that is supported by our expression data. Alternatively, CNS neurons may directly interact with infiltrating immune cell populations by altering their survival or causing alteration of their effector phenotype. Recently, isolated neurons were found to enhance the proliferation of CD4$^+$ T cells in a MHC class II-independent, TGF-β1- and B7-dependent way and to convert encephalitogenic T cell lines to CD25$^+$TGF-β1$^+$CTLA-4$^+$FoxP3$^+$ T regulatory cells that suppress encephalitogenic T cells and inhibit EAE (13). In this study, we did not find support for such a mechanism being driven by NF-κB in neurons in vivo since changes in the proportions of CD25$^+$FoxP3$^+$ T regulatory cells did not parallel those of CD4$^+$ IFN-γ^+ cells in nIKKβKO spinal cord. Interestingly, previous studies of the role of neuronal NF-κB in the CNS of mice have revealed a deleterious role in acute injury caused by cerebral ischemia (30, 31). Also, astroglial and astroglial/neuronal NF-κB had deleterious effects by enhancing gliosis and chronic CNS inflammation in EAE (32, 33). Taken together, these results have supported the idea that NF-κB may be a good therapeutic target for the treatment of acute CNS pathologies like stroke and chronic ones like MS. However, the results of the present study show that NF-κB also becomes activated in neurons to mediate neuroprotection during chronic diseases like MS and caution that any future therapeutic targeting of NF-κB in the CNS must take into account cell specificity of effect and the type of neurodegeneration.

The findings of this study contribute to the understanding of how the CNS and the immune system interact during the development of CNS inflammation and autoimmunity. Our data show that neuron control of CNS immune function extends beyond a role in the maintenance of immune privilege in the normal healthy CNS to the active protection of CNS tissues

during CNS inflammation and autoimmunity. Our finding that neuron integrity has an anti-inflammatory effect during the development of autoimmune disease may have important consequences for therapy in MS and emphasizes the importance of neuroprotective strategies as a major goal not only for directly preserving neurons and axons but also for indirectly suppressing the pathogenic CNS-directed autoimmune and inflammatory processes.

Supplementary Material

Refer to Web version on PubMed Central for supplementary material.

Acknowledgments

We thank Hartmut Wekerle and Gurumoorthy Krishnamoorthy for teaching us CNS lymphocyte isolation, Maria Evangelidou and Stavroula Alexopoulou for help with animal experiments, and Vasso Kyrargyri for help with the confocal microscope. We also thank Burkhard Becher for critically reading this manuscript.

References

1. Sospedra M, Martin R. Immunology of multiple sclerosis. Annu Rev Immunol. 2005; 23:683–747. [PubMed: 15771584]
2. Dutta R, Trapp BD. Pathogenesis of axonal and neuronal damage in multiple sclerosis. Neurology. 2007; 68:S22–S31. [PubMed: 17548565]
3. Lassmann H. New concepts on progressive multiple sclerosis. Curr Neurol Neurosci Rep. 2007; 7:239–244. [PubMed: 17488590]
4. Hohlfeld R, Kerschensteiner M, Stadelmann C, Lassmann H, Wekerle H. The neuroprotective effect of inflammation: implications for the therapy of multiple sclerosis. Neurol Sci. 2006; 27(Suppl 1):S1–S7. [PubMed: 16708174]
5. Trapp BD, Nave KA. Multiple sclerosis: an immune or neurodegenerative disorder? Annu Rev Neurosci. 2008; 31:247–269. [PubMed: 18558855]
6. Neumann H, Wekerle H. Neuronal control of the immune response in the central nervous system: linking brain immunity to neurodegeneration. J Neuropathol Exp Neurol. 1998; 57:1–9. [PubMed: 9600191]
7. Neumann H, Schmidt H, Cavalie A, Jenne D, Wekerle H. Major histocompatibility complex (MHC) class I gene expression in single neurons of the central nervous system: differential regulation by interferon (IFN)-γ and tumor necrosis factor (TNF)-α. J Exp Med. 1997; 185:305–316. [PubMed: 9016879]
8. Hoek RM, Ruuls SR, Murphy CA, Wright GJ, Goddard R, Zurawski SM, Blom B, Homola ME, Streit WJ, Brown MH, et al. Down-regulation of the macrophage lineage through interaction with OX2 (CD200). Science. 2000; 290:1768–1771. [PubMed: 11099416]
9. Mott RT, Ait-Ghezala G, Town T, Mori T, Vendrame M, Zeng J, Ehrhart J, Mullan M, Tan J. Neuronal expression of CD22: novel mechanism for inhibiting microglial proinflammatory cytokine production. Glia. 2004; 46:369–379. [PubMed: 15095367]
10. Flugel A, Schwaiger FW, Neumann H, Medana I, Willem M, Wekerle H, Kreutzberg GW, Graeber MB. Neuronal FasL induces cell death of encephalitogenic T lymphocytes. Brain Pathol. 2000; 10:353–364. [PubMed: 10885654]
11. Tian L, Yoshihara Y, Mizuno T, Mori K, Gahmberg CG. The neuronal glycoprotein telencephalin is a cellular ligand for the CD11a/CD18 leukocyte integrin. J Immunol. 1997; 158:928–936. [PubMed: 8993013]
12. Tian L, Kilgannon P, Yoshihara Y, Mori K, Gallatin WM, Carpen O, Gahmberg CG. Binding of T lymphocytes to hippocampal neurons through ICAM-5 (telencephalin) and characterization of its interaction with the leukocyte integrin CD11a/CD18. Eur J Immunol. 2000; 30:810–818. [PubMed: 10741396]

13. Liu Y, Teige I, Birnir B, Issazadeh-Navikas S. Neuron-mediated generation of regulatory T cells from encephalitogenic T cells suppresses EAE. Nat Med. 2006; 12:518–525. [PubMed: 16633347]
14. Cheng B, Christakos S, Mattson MP. Tumor necrosis factors protect neurons against metabolic-excitotoxic insults and promote maintenance of calcium homeostasis. Neuron. 1994; 12:139–153. [PubMed: 7507336]
15. Bruce AJ, Boling W, Kindy MS, Peschon J, Kraemer PJ, Carpenter MK, Holtsberg FW, Mattson MP. Altered neuronal and microglial responses to excitotoxic and ischemic brain injury in mice lacking TNF receptors. Nat Med. 1996; 2:788–794. [PubMed: 8673925]
16. Taoufik E, Valable S, Muller GJ, Roberts ML, Divoux D, Tinel A, Voulgari-Kokota A, Tseveleki V, Altruda F, Lassmann H, et al. $FLIP_L$ protects neurons against in vivo ischemia and in vitro glucose deprivation-induced cell death. J Neurosci. 2007; 27:6633–6646. [PubMed: 17581950]
17. Lambertsen KL, Clausen BH, Babcock AA, Gregersen R, Fenger C, Nielsen HH, Haugaard LS, Wirenfeldt M, Nielsen M, Dagnaes-Hansen F, et al. Microglia protect neurons against ischemia by synthesis of tumor necrosis factor. J Neurosci. 2009; 29:1319–1330. [PubMed: 19193879]
18. Taoufik E, Petit E, Divoux D, Tseveleki V, Mengozzi M, Roberts ML, Valable S, Ghezzi P, Quackenbush J, Brines M, et al. TNF receptor I sensitizes neurons to erythropoietin- and VEGF-mediated neuroprotection after ischemic and excitotoxic injury. Proc Natl Acad Sci USA. 2008; 105:6185–6190. [PubMed: 18413601]
19. Li Q I, Verma M. NF-κB regulation in the immune system. Nat Rev Immunol. 2002; 2:725–734. [PubMed: 12360211]
20. Karin M, Lin A. NF-κB at the crossroads of life and death. Nat Immunol. 2002; 3:221–227. [PubMed: 11875461]
21. Rius J, Guma M, Schachtrup C, Akassoglou K, Zinkernagel AS, Nizet V, Johnson RS, Haddad GG, Karin M. NF-κB links innate immunity to the hypoxic response through transcriptional regulation of HIF-1α. Nature. 2008; 453:807–811. [PubMed: 18432192]
22. Ghosh S, Karin M. Missing pieces in the NF-κB puzzle. Cell. 2002; 109(Suppl):S81–S96. [PubMed: 11983155]
23. Meffert MK, Chang JM, Wiltgen BJ, Fanselow MS, Baltimore D. NF-κB functions in synaptic signaling and behavior. Nat Neurosci. 2003; 6:1072–1078. [PubMed: 12947408]
24. Albensi BC, Mattson MP. Evidence for the involvement of TNF and NF-κB in hippocampal synaptic plasticity. Synapse. 2000; 35:151–159. [PubMed: 10611641]
25. Kaltschmidt B, Ndiaye D, Korte M, Pothion S, Arbibe L, Prullage M, Pfeiffer J, Lindecke A, Staiger V, Israel A, et al. NF-κB regulates spatial memory formation and synaptic plasticity through protein kinase A/CREB signaling. Mol Cell Biol. 2006; 26:2936–2946. [PubMed: 16581769]
26. Schneider A, Martin-Villalba A, Weih F, Vogel J, Wirth T, Schwaninger M. NF-κB is activated and promotes cell death in focal cerebral ischemia. Nat Med. 1999; 5:554–559. [PubMed: 10229233]
27. Mattson MP, Goodman Y, Luo H, Fu W, Furukawa K. Activation of NF-κB protects hippocampal neurons against oxidative stress-induced apoptosis: evidence for induction of manganese superoxide dismutase and suppression of peroxynitrite production and protein tyrosine nitration. J Neurosci Res. 1997; 49:681–697. [PubMed: 9335256]
28. Bhakar AL, Tannis LL, Zeindler C, Russo MP, Jobin C, Park DS, MacPherson S, Barker PA. Constitutive nuclear factor-κB activity is required for central neuron survival. J Neurosci. 2002; 22:8466–8475. [PubMed: 12351721]
29. Fridmacher V, Kaltschmidt B, Goudeau B, Ndiaye D, Rossi FM, Pfeiffer J, Kaltschmidt C, Israel A, Memet S. Forebrain-specific neuronal inhibition of nuclear factor-κB activity leads to loss of neuroprotection. J Neurosci. 2003; 23:9403–9408. [PubMed: 14561868]
30. Herrmann O, Baumann B, de Lorenzi R, Muhammad S, Zhang W, Kleesiek J, Malfertheiner M, Kohrmann M, Potrovita I, Maegele I, et al. IKK mediates ischemia-induced neuronal death. Nat Med. 2005; 11:1322–1329. [PubMed: 16286924]
31. Zhang W, Potrovita I, Tarabin V, Herrmann O, Beer V, Weih F, Schneider A, Schwaninger M. Neuronal activation of NF-κB contributes to cell death in cerebral ischemia. J Cereb Blood Flow Metab. 2005; 25:30–40. [PubMed: 15678110]

32. van Loo G, De Lorenzi R, Schmidt H, Huth M, Mildner A, Schmidt-Supprian M, Lassmann H, Prinz MR, Pasparakis M. Inhibition of transcription factor NF-κB in the central nervous system ameliorates autoimmune encephalomyelitis in mice. Nat Immunol. 2006; 7:954–961. [PubMed: 16892069]
33. Brambilla R, Persaud T, Hu X, Karmally S, Shestopalov VI, Dvoriantchikova G, Ivanov D, Nathanson L, Barnum SR, Bethea JR. Transgenic inhibition of astroglial NF-κB improves functional outcome in experimental autoimmune encephalomyelitis by suppressing chronic central nervous system inflammation. J Immunol. 2009; 182:2628–2640. [PubMed: 19234157]
34. Youssef S, Steinman L. At once harmful and beneficial: the dual properties of NF-κB. Nat Immunol. 2006; 7:901–902. [PubMed: 16924250]
35. Park JM, Greten FR, Li ZW, Karin M. Macrophage apoptosis by anthrax lethal factor through p38 MAP kinase inhibition. Science. 2002; 297:2048–2051. [PubMed: 12202685]
36. Li ZW, Omori SA, Labuda T, Karin M, Rickert RC. IKKβ is required for peripheral B cell survival and proliferation. J Immunol. 2003; 170:4630–4637. [PubMed: 12707341]
37. Minichiello L, Korte M, Wolfer D, Kuhn R, Unsicker K, Cestari V, Rossi-Arnaud C, Lipp HP, Bonhoeffer T, Klein R. Essential role for TrκB receptors in hippocampus-mediated learning. Neuron. 1999; 24:401–414. [PubMed: 10571233]
38. Soriano P. Generalized *lacZ* expression with the ROSA26 Cre reporter strain. Nat Genet. 1999; 21:70–71. [PubMed: 9916792]
39. Tselios T, Probert L, Daliani I, Matsoukas E, Troganis A, Gerothanassis IP, Mavromoustakos T, Moore GJ, Matsoukas JM. Design and synthesis of a potent cyclic analogue of the myelin basic protein epitope MBP72–85: importance of the Ala^{81} carboxyl group and of a cyclic conformation for induction of experimental allergic encephalomyelitis. J Med Chem. 1999; 42:1170–1177. [PubMed: 10197961]
40. Tselios T, Daliani I, Deraos S, Thymianou S, Matsoukas E, Troganis A, Gerothanassis I, Mouzaki A, Mavromoustakos T, Probert L, Matsoukas J. Treatment of experimental allergic encephalomyelitis (EAE) by a rationally designed cyclic analogue of myelin basic protein (MBP) epitope 72–85. Bioorg Med Chem Lett. 2000; 10:2713–2717. [PubMed: 11133075]
41. Tseveleki V, Bauer J, Taoufik E, Ruan C, Leondiadis L, Haralambous S, Lassmann H, Probert L. Cellular FLIP (long isoform) overexpression in T cells drives Th2 effector responses and promotes immunoregulation in experimental autoimmune encephalomyelitis. J Immunol. 2004; 173:6619–6626. [PubMed: 15557152]
42. Krishnamoorthy G, Lassmann H, Wekerle H, Holz A. Spontaneous opticospinal encephalomyelitis in a double-transgenic mouse model of autoimmune T cell/B cell cooperation. J Clin Invest. 2006; 116:2385–2392. [PubMed: 16955140]
43. Rossler K, Neuchrist C, Kitz K, Scheiner O, Kraft D, Lassmann H. Expression of leucocyte adhesion molecules at the human blood-brain barrier (BBB). J Neurosci Res. 1992; 31:365–374. [PubMed: 1374132]
44. Nicole O, Ali C, Docagne F, Plawinski L, MacKenzie ET, Vivien D, Buisson A. Neuroprotection mediated by glial cell line-derived neurotrophic factor: involvement of a reduction of NMDA-induced calcium influx by the mitogen-activated protein kinase pathway. J Neurosci. 2001; 21:3024–3033. [PubMed: 11312287]
45. Koh JY, Choi DW. Effect of anticonvulsant drugs on glutamate neurotoxicity in cortical cell culture. Neurology. 1987; 37:319–322. [PubMed: 3808315]
46. Kornek B, Storch MK, Bauer J, Djamshidian A, Weissert R, Wallstroem E, Stefferl A, Zimprich F, Olsson T, Linington C, et al. Distribution of a calcium channel subunit in dystrophic axons in multiple sclerosis and experimental autoimmune encephalomyelitis. Brain. 2001; 124:1114–1124. [PubMed: 11353727]
47. Brand-Schieber E, Werner P. Calcium channel blockers ameliorate disease in a mouse model of multiple sclerosis. Exp Neurol. 2004; 189:5–9. [PubMed: 15296830]
48. Sheldon RA, Osredkar D, Lee CL, Jiang X, Mu D, Ferriero DM. HIF-1α-deficient mice have increased brain injury after neonatal hypoxiaischemia. Dev Neurosci. 2009; 31:452–458. [PubMed: 19672073]

49. Gold R, Linington C, Lassmann H. Understanding pathogenesis and therapy of multiple sclerosis via animal models: 70 years of merits and culprits in experimental autoimmune encephalomyelitis research. Brain. 2006; 129:1953–1971. [PubMed: 16632554]
50. Kreuz S, Siegmund D, Scheurich P, Wajant H. NF-κB inducers upregulate cFLIP, a cycloheximide-sensitive inhibitor of death receptor signaling. Mol Cell Biol. 2001; 21:3964–3973. [PubMed: 11359904]
51. Karin M, Yamamoto Y, Wang QM. The IKK NF-κB system: a treasure trove for drug development. Nat Rev Drug Discov. 2004; 3:17–26. [PubMed: 14708018]
52. Mattson MP, Camandola S. NF-κB in neuronal plasticity and neurodegenerative disorders. J Clin Invest. 2001; 107:247–254. [PubMed: 11160145]
53. Kaltschmidt B, Widera D, Kaltschmidt C. Signaling via NF-κB in the nervous system. Biochim Biophys Acta. 2005; 1745:287–299. [PubMed: 15993497]
54. Schmidt D, Textor B, Pein OT, Licht AH, Andrecht S, Sator-Schmitt M, Fusenig NE, Angel P, Schorpp-Kistner M. Critical role for NF- κB-induced JunB in VEGF regulation and tumor angiogenesis. EMBO J. 2007; 26:710–719. [PubMed: 17255940]
55. Bernaudin M, Nedelec AS, Divoux D, MacKenzie ET, Petit E, Schumann-Bard P. Normobaric hypoxia induces tolerance to focal permanent cerebral ischemia in association with an increased expression of hypoxia-inducible factor-1 and its target genes, erythropoietin and VEGF, in the adult mouse brain. J Cereb Blood Flow Metab. 2002; 22:393–403. [PubMed: 11919510]
56. Jin KL, Mao XO, Greenberg DA. Vascular endothelial growth factor: direct neuroprotective effect in in vitro ischemia. Proc Natl Acad Sci USA. 2000; 97:10242–10247. [PubMed: 10963684]
57. Sun Y, Jin K, Xie L, Childs J, Mao XO, Logvinova A, Greenberg DA. VEGF-induced neuroprotection, neurogenesis, and angiogenesis after focal cerebral ischemia. J Clin Invest. 2003; 111:1843–1851. [PubMed: 12813020]
58. Zheng C, Nennesmo I, Fadeel B, Henter JI. Vascular endothelial growth factor prolongs survival in a transgenic mouse model of ALS. Ann Neurol. 2004; 56:564–567. [PubMed: 15389897]
59. Storkebaum E, Lambrechts D, Dewerchin M, Moreno-Murciano MP, Appelmans S, Oh H, Van Damme P, Rutten B, Man WY, De Mol M, et al. Treatment of motoneuron degeneration by intracerebroventricular delivery of VEGF in a rat model of ALS. Nat Neurosci. 2005; 8:85–92. [PubMed: 15568021]
60. Wang Y, Berezovska O, Fedoroff S. Expression of colony stimulating factor-1 receptor (CSF-1R) by CNS neurons in mice. J Neurosci Res. 1999; 57:616–632. [PubMed: 10462686]
61. Jelinsky SA, Miyashiro JS, Saraf KA, Tunkey C, Reddy P, Newcombe J, Oestreicher JL, Brown E, Trepicchio WL, Leonard JP, Marusic S. Exploiting genotypic differences to identify genes important for EAE development. J Neurol Sci. 2005; 239:81–93. [PubMed: 16214174]
62. Michaelson MD, Bieri PL, Mehler MF, Xu H, Arezzo JC, Pollard JW, Kessler JA. CSF-1 deficiency in mice results in abnormal brain development. Development. 1996; 122:2661–2672. [PubMed: 8787741]
63. Berezovskaya O, Maysinger D, Fedoroff S. The hematopoietic cytokine, colony-stimulating factor 1, is also a growth factor in the CNS: congenital absence of CSF-1 in mice results in abnormal microglial response and increased neuron vulnerability to injury. Int J Dev Neurosci. 1995; 13:285–299. [PubMed: 7572282]
64. Berezovskaya O, Maysinger D, Fedoroff S. Colony stimulating factor- 1 potentiates neuronal survival in cerebral cortex ischemic lesion. Acta Neuropathol. 1996; 92:479–486. [PubMed: 8922060]
65. Biber K, Neumann H, Inoue K, Boddeke HW. Neuronal “On” and “Off” signals control microglia. Trends Neurosci. 2007; 30:596–602. [PubMed: 17950926]
66. Brionne TC, Tesseur I, Masliah E, Wyss-Coray T. Loss of TGF-β1 leads to increased neuronal cell death and microgliosis in mouse brain. Neuron. 2003; 40:1133–1145. [PubMed: 14687548]
67. Neumann H, Cavalie A, Jenne DE, Wekerle H. Induction of MHC class I genes in neurons. Science. 1995; 269:549–552. [PubMed: 7624779]
68. Neumann H, Misgeld T, Matsumuro K, Wekerle H. Neurotrophins inhibit major histocompatibility class II inducibility of microglia: involvement of the p75 neurotrophin receptor. Proc Natl Acad Sci USA. 1998; 95:5779–5784. [PubMed: 9576961]

69. Majed HH, Chandran S, Niclou SP, Nicholas RS, Wilkins A, Wing MG, Rhodes KE, Spillantini MG, Compston A. A novel role for Sema3A in neuroprotection from injury mediated by activated microglia. J Neurosci. 2006; 26:1730–1738. [PubMed: 16467521]
70. Savarin-Vuaillat C, Ransohoff RM. Chemokines and chemokine receptors in neurological disease: raise, retain, or reduce? Neurotherapeutics. 2007; 4:590–601. [PubMed: 17920540]
71. Carlson T, Kroenke M, Rao P, Lane TE, Segal B. The Th17-ELR^{+} CXC chemokine pathway is essential for the development of central nervous system autoimmune disease. J Exp Med. 2008; 205:811–823. [PubMed: 18347102]
72. Kroenke MA, Carlson TJ, Andjelkovic AV, Segal BM. IL-12- and IL-23-modulated T cells induce distinct types of EAE based on histology, CNS chemokine profile, and response to cytokine inhibition. J Exp Med. 2008; 205:1535–1541. [PubMed: 18573909]
73. Segal BM. The role of natural killer cells in curbing neuroinflammation. J Neuroimmunol. 2007; 191:2–7. [PubMed: 17904646]
74. Fontaine V, Mohand-Said S, Hanoteau N, Fuchs C, Pfizenmaier K, Eisel U. Neurodegenerative and neuroprotective effects of tumor Necrosis factor (TNF) in retinal ischemia: opposite roles of TNF receptor 1 and TNF receptor 2. J Neurosci. 2002; 22:RC216. [PubMed: 11917000]
75. Marchetti L, Klein M, Schlett K, Pfizenmaier K, Eisel UL. Tumor necrosis factor (TNF)-mediated neuroprotection against glutamate-induced excitotoxicity is enhanced by *N*-methyl-D-aspartate receptor activation: essential role of a TNF receptor 2-mediated phosphatidylinositol 3-kinase-dependent NF-κB pathway. J Biol Chem. 2004; 279:32869–32881. [PubMed: 15155767]

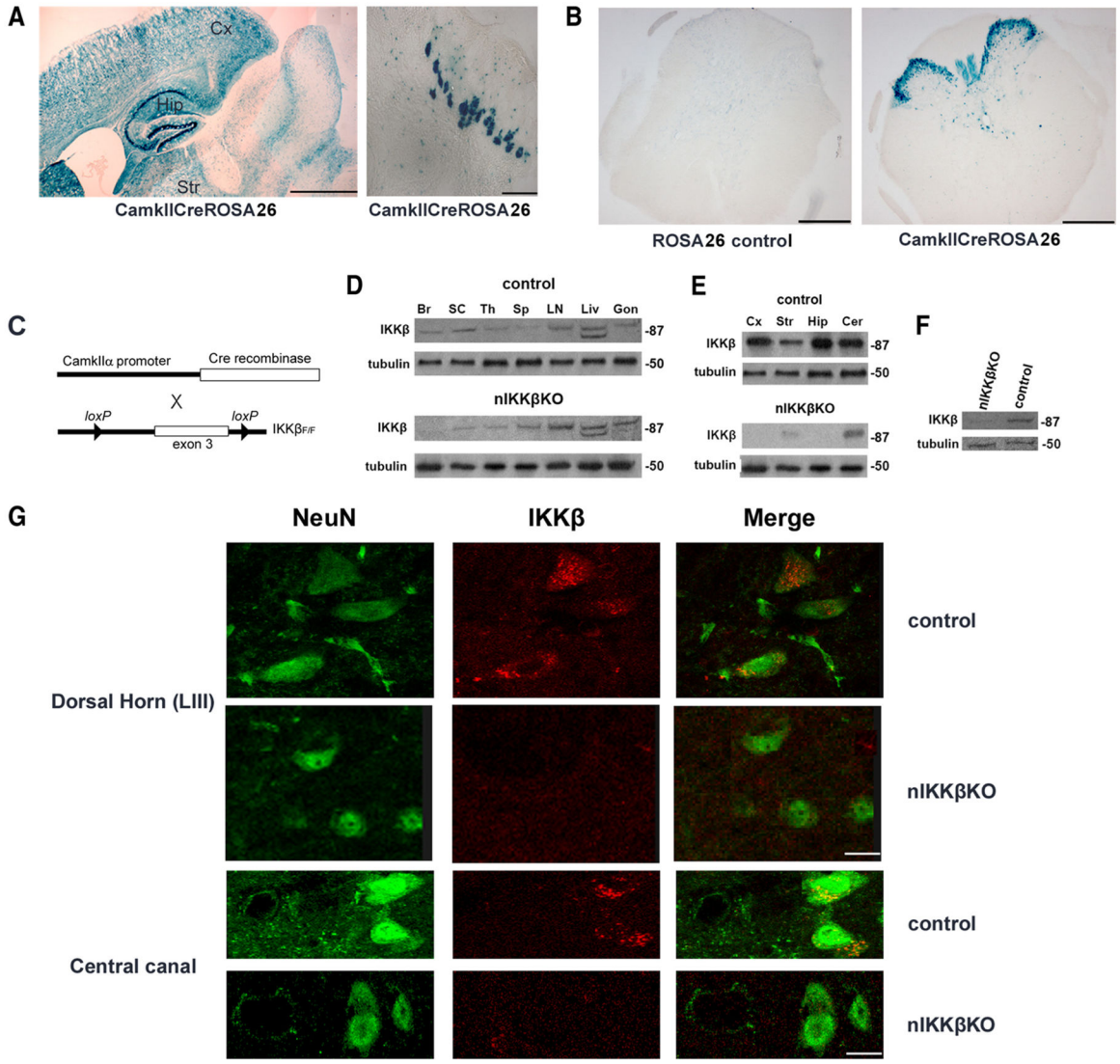

FIGURE 1.

IKK*β* is selectively deleted in CNS neurons of nIKK*β*KO mice. *A*, CamkIICre-mediated gene deletion in CNS neurons was confirmed using ROSA26 reporter mice that carry a *loxP*-flanked (floxed, F) neo cassette within *lacZ*. Cre-mediated activation of *lacZ*, detected by staining with X-Gal, was widespread in cells of the cortex (Cx), hippocampus (Hip), and striatum (Str; *left panel*) as well as Purkinje cells of the cerebellum (Cer; *right panel*). *B*, X-Gal staining was also detected in cells localized in the outer laminas (especially laminas II and III) of the dorsal horn, around the central canal (lamina X), and in sparse cells in the ventral horn of the spinal cord, as shown in sections from the lumbar region. *C*, Scheme showing the strategy for the generation of nIKK*β*KO mice. *D*, The expression of IKK*β* was selectively depleted in brain and spinal cord of nIKK*β*KO mice as determined by Western blot. Br, Brain; SC, spinal cord; Th, thymus; Sp, spleen; Liv, liver; Gon, gonads. *E*, IKK*β* expression was completely depleted in the cortex and hippocampus and significantly depleted in the striatum (Str) and cerebellum of nIKK*β*KO mice as shown by Western blot.

F, The contribution of neurons to IKKβ depletion was demonstrated by Western blot of cell extracts from highly enriched cultures (>95%) of nIKKβKO and control cortical neurons. *G*, Immunofluorescent staining of sections from lumbar spinal cords of nIKKβKO and control mice for NeuN (green, *left panel*) and IKKβ (red, *central panel*). Colocalization of NeuN and IKKβ (*right panel*) was observed in neurons throughout the gray matter, including pyramidal cells of lamina III and lateral to the central canal, in control but not nIKKβKO spinal cord. Images are representative of two independent experiments. Scale bars: *A*, 1 mm (*left panel*); 100 μm (*right panel*); *C*, 1 mm; and *G*, 10 μm.

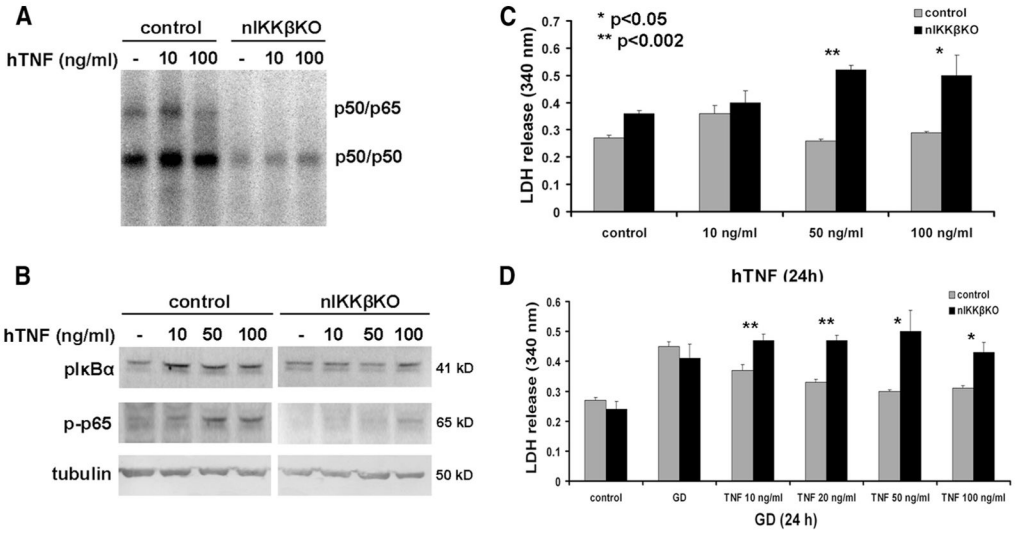

FIGURE 2.

nIKK*β*KO neurons are sensitive to TNF toxicity and resistant to TNF-mediated neuroprotection against GD. *A*, Treatment of cortical neurons with hTNF for 20 min induced p50/p65 activity in control, but not nIKK*β*KO, neurons as assessed by EMSA. *B*, Treatment of cortical neurons with hTNF for 20 min induced expression of the phosphorylated forms of I*κ*B*α* and p65 in control, but not nIKK*β*KO, neurons as assessed by Western blot. *C*, Treatment of neurons with hTNF induced cytotoxicity in nIKK*β*KO, but not control, neurons in a dose-dependent manner as measured by increased LDH release (results shown represent mean LDH release ± SEM of triplicate samples from two independent experiments). *D*, Dose-dependent TNF-mediated neuroprotection against GD (24 h) observed in control neurons was abolished in nIKK*β*KO neurons, as measured by LDH release (results shown represent the mean LDH release ± SEM of duplicate samples from two independent experiments).

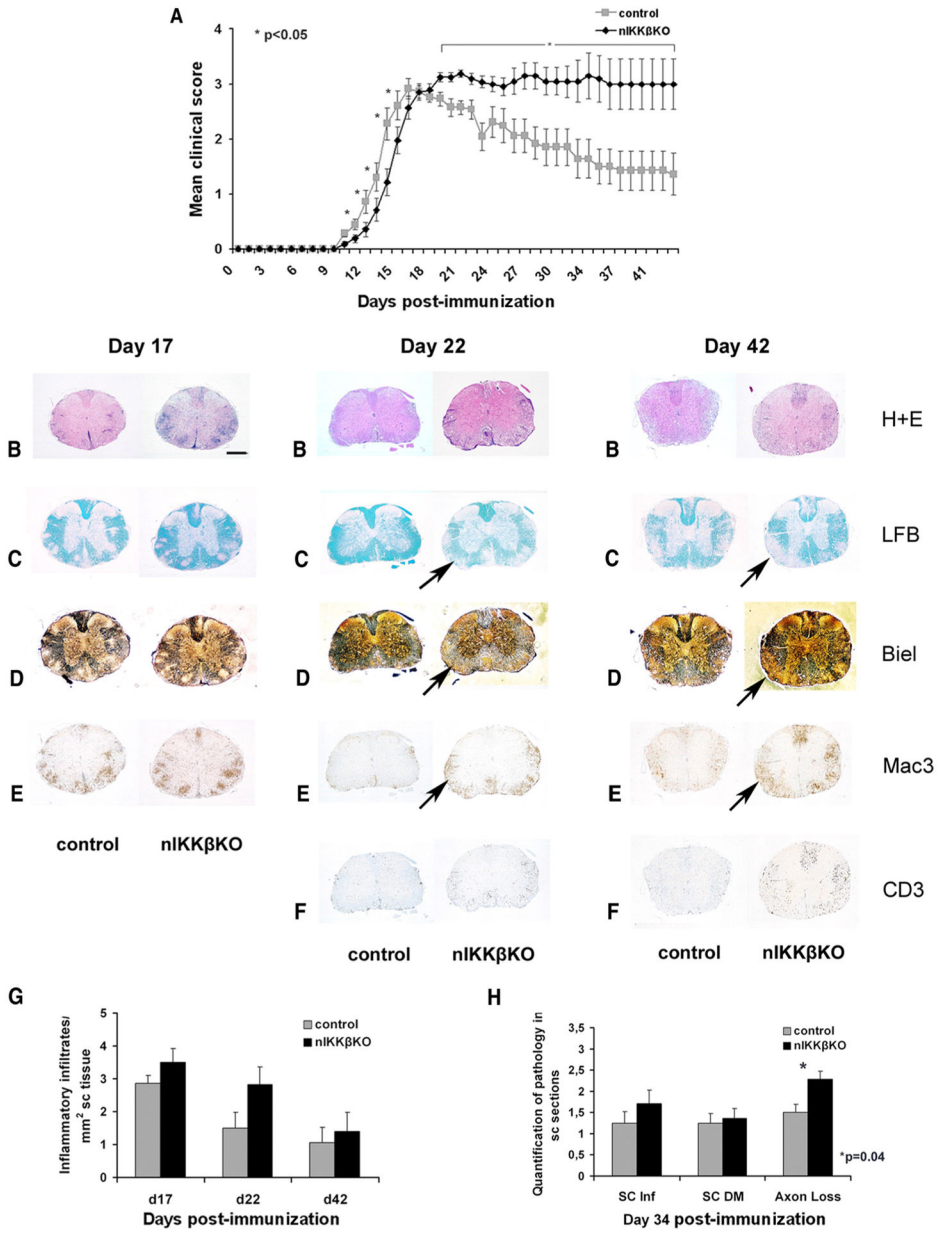

FIGURE 3.

nIKK*β*KO mice develop a severe, nonresolving form of $MOG_{35–55}$-EAE with enhanced inflammation and axon loss in the spinal cord compared with control mice. *A*, Mean clinical scores for nIKK*β*KO ($n = 20$) and control mice ($n = 20$) after immunization with $MOG_{35–55}$ peptide. Results shown are representative of three independent experiments (experiment 3) (see Table I) and are presented as mean values ± SEM. *B–F*, Spinal cord sections from nIKK*β*KO and control mice taken at days 17, 22, and 42 after immunization and stained with H&E (*B*), Luxol fast blue (*C*), Bielschowsky silver stain (*D*), anti-Mac3 (*E*), and anti-CD3 (*F*). At day 17 after immunization, spinal cords from nIKK*β*KO and control mice showed similar neuropathological changes with severe meningeal and parenchymal inflammation (*B* and *E*), demyelination (*C*), and axonal damage (*D*). At days 22 and 42 after

immunization, spinal cords from nIKKβKO showed severe persistent demyelination (*C*, black arrow), axonal damage (*D*, black arrow), and inflammation (*E*, black arrow) including the presence of large numbers of CD3-immunoreactive T cells (*F*). Scale bar, 1 mm. *G*, Quantitative representation of inflammatory infiltrates in nIKKβKO and control spinal cord at days 17, 22, and 42 after immunization. Inflammation was scored as inflammatory infiltrates per mm^2 of tissue. *H*, Quantification of spinal cord inflammation, demyelination, and axon loss on day 34 after immunization. Demyelination was scored in H&E-stained sections as follows: 0.5 for few perivascular demyelinated fibers, 1 for perivascular demyelination, and 2 for confluent and subpial demyelination. Axon loss was assessed depending on the percentage of loss: 1 for 0–30%, 2 for 30–60%, and 3 for >60%.

A

Cytokines	Mean fold change ±S.E.M.	p value	Cytokines	Mean fold change ±S.E.M.	p value
Adaptive immunity			*Chemokines*		
CD30L	**1.19 ±0.09**	p<0.05	KC / CXCL1	**1.84 ±0.01**	p<0.001
IL-12 p40/p70	**2.52 ±0.69**	p<0.05	MCP-1 / CCL2	**1.11 ±0.001**	p<0.01
IL-12 p70	**1.29 ±0.05**	p<0.05	RANTES / CCL5	**1.12 ±0.001**	p<0.01
IL-17	**2.29 ±0.61**	p<0.05	CTACK / CCL27	**1.21 ±0.003**	p<0.02
IL-10	0.78 ±0.07	p<0.05	TECK / CCL25	**1.63 ±0.03**	p<0.04
Growth factors			CXCL16	**2.50 ±0.42**	p<0.05
GM-CSF	**1.20 ±0.02**	p<0.02	MCP-5 / CCL12	**1.27 ±0.14**	p<0.05
Thrombopoietin	**1.62 ±0.02**	p<0.05	MIP-1α / CCL3	**1.10 ±0.02**	p<0.05
VEGF	0.42 ±0.02	p<0.02	TARC / CCL17	**1.62 ±0.13**	p<0.05
Axl	0.67 ±0.01	p<0.02	TCA-3 / CCL1	**1.47 ±0.14**	p<0.05
Innate Immunity-Inflammation			MIG / CXCL9	0.85 ±0.002	p<0.02
IL-6	**1.28 ±0.07**	p<0.02	Eotaxin / CCL11	0.80 ±0.06	p<0.05
sTNF receptor II	**1.20 ±0.07**	p<0.02	*Others*		
TNF	**2.04 ±0.16**	p<0.02	Leptin receptor	**1.78 ±0.20**	p<0.05
sTNF receptor I	**1.46 ±0.10**	p<0.05	TIMP-1	**1.45 ±0.17**	p<0.05

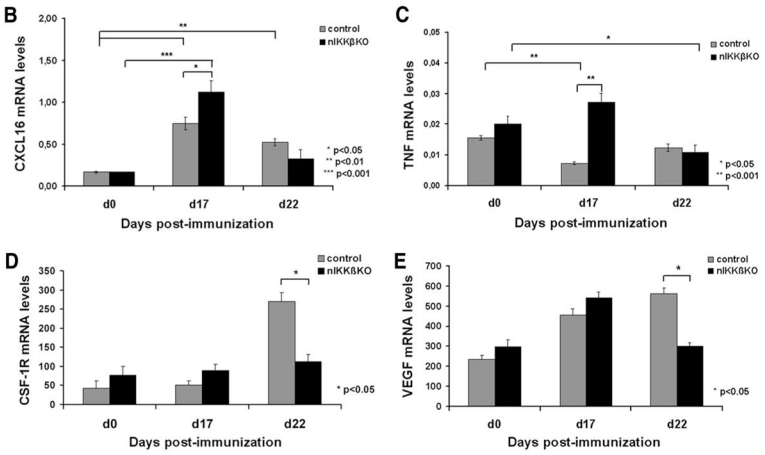

FIGURE 4.

Enhanced production of proinflammatory cytokines and chemokines and reduced production of neuroprotective factors in the spinal cord of nIKK*β*KO EAE mice. *A*, Differential production of immune mediators in protein lysates from nIKK*β*KO ($n = 2$) compared with control ($n = 2$) spinal cord taken on day 22 after immunization as measured by a mouse cytokine Ab array (Chemicon International). Results are presented as the mean fold change ± SEM in cytokine production in spinal cords taken from two independent experiments. *B*–*E*, Differential expression of immune genes in total mRNA isolates taken from nIKK*β*KO and control spinal cord before and after EAE induction as measured by RT-PCR. mRNA levels of CXCL16 (*B*) and TNF (*C*) were measured by quantitative RT-PCR, and mRNA levels of CSF-1R (*D*) and VEGF (*E*) by semiquantitative RT-PCR in nIKK*β*KO and control spinal cords (day 0 (nonimmunized): control, $n = 2$ and nIKK*β*KO, $n = 2$; day 17: control, $n = 2$ and nIKK*β*KO, $n = 2$; day 22: control, $n = 2$ and nIKK*β*KO, $n = 3$).

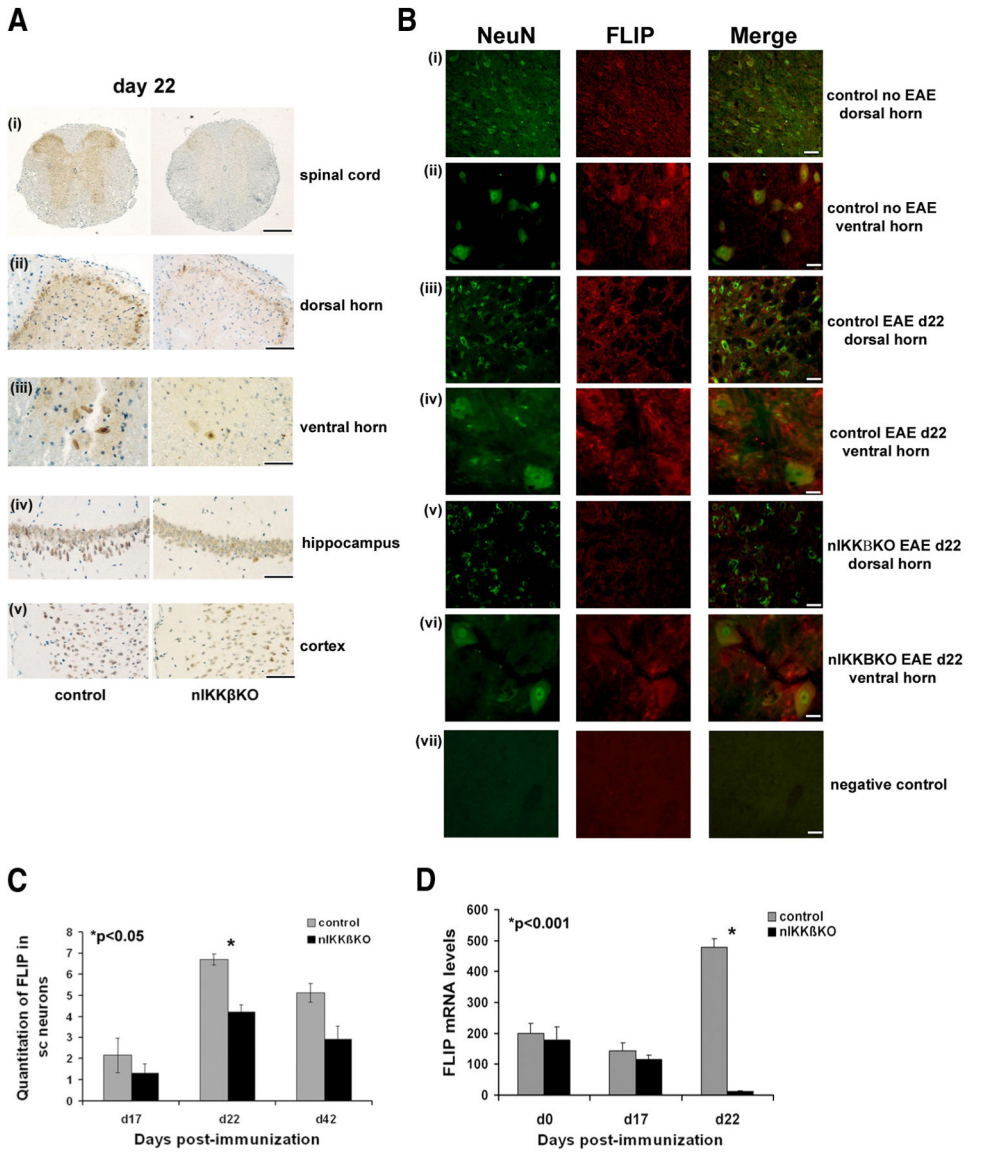

FIGURE 5.

nIKK*β*KO mice fail to maintain or induce production of the neuroprotective protein FLIP in the spinal cord during EAE. *A*, Localization of $FLIP_{S/L}$ immunoreactivity in the spinal cord and brain of nIKK*β*KO and control mice at day 22 after immunization. Low levels of $FLIP_{S/L}$ expression were observed in spinal cord sections (*Ai*) from nIKK*β*KO mice notably in the dorsal (*ii*) and ventral horns (*iii*). $FLIP_{S/L}$ expression levels in hippocampus (*iv*) and cortex (*v*) were more pronounced in control mice compared with nIKK*β*KO mice. There was also weak expression of $FLIP_{S/L}$ in inflammatory cells (data not shown). *B*, Immunofluorescence localization of NeuN (green, *left panel*) and $FLIP_{S/L}$ (red, *central panel*) in lumbar spinal cords of nIKK*β*KO and control nonimmunized or day 22 of EAE mice. Colocalization of NeuN and $FLIP_{S/L}$ (*right panel*) was observed in neurons of the dorsal (*i*, *iii*, and *v*) and ventral horns (*ii*, *iv*, and *vi*) of the spinal cord prior to and during EAE. Reduced levels of $FLIP_{S/L}$ immunoreactivity were observed in the nIKK*β*KO spinal

cord (*v* and *vi*). (*vii*, negative control with omission of primary Abs). *C*, Quantitative assessment of the numbers of $FLIP_{S/L}$ immunoreactive neurons in the spinal cord of nIKK*β*KO and control mice at different time points after immunization. Values are numbers of positive cells/mm^2 tissue. *D*, Semiquantitative RT-PCR analysis of FLIP mRNA levels in nIKK*β*KO and control spinal cord following EAE (day 0 (nonimmunized): control, $n = 2$ and nIKK*β*KO, $n = 2$; day 17: control, $n = 2$ and nIKK*β*KO, $n = 2$; day 22: control, $n = 2$ and nIKK*β*KO, $n = 3$). Scale bars: *Ai*, 1 mm; *Aii* and *Bvii*, 100 *μ*m; *Aiii* and *B*, *i–iii* and *v*, 50 *μ*m; *A*, *iv* and *v*, 500 *μ*m; and *B*, *ii–iv* and *vi*,10 *μ*m.

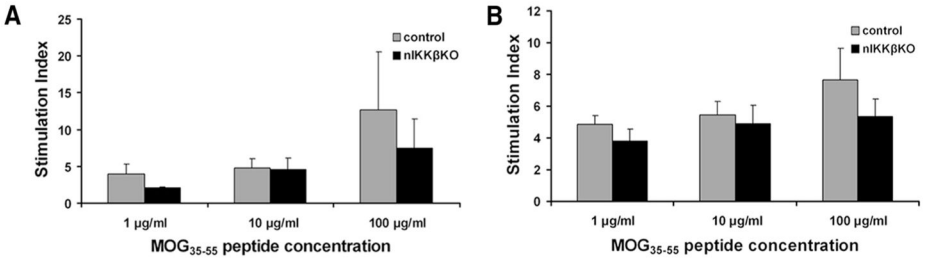

C

	Peak of disease (d17)			Chronic Phase (d38)		
Cell markers	control	nIKKβKO	p	control	nIKKβKO	p
CD4+	20,8 ± 3,17 %	28.8 ± 3,36 %	**0.006**	6,59 ± 1,47 %	9,92 ± 0,97 %	**0.04**
CD8+	4,18 ± 1,20 %	2,73 ± 0,25 %	0.20	4,93 ± 1,08 %	4,20 ± 1,05 %	0.18
B220+	33,98 ± 4,51 %	34,39 ± 16,26 %	0.49	2,83 ± 0,64 %	2,09 ± 1,00 %	0.36
NK1.1+	46,24 ± 3,36 %	32,54 ± 2,05 %	**0.03**	1,81 ± 0,06 %	1,20 ± 0,06 %	**0.015**
CD11b+	18,28 ± 1,40 %	20,43 ± 0,50 %	0.06	13,90 ± 4,48 %	10,38 ± 2,43 %	0.14

D

	Peak of disease (d17)			Chronic Phase (d38)		
Draining LN cells	control	nIKKβKO	p	control	nIKKβKO	p
CD4+ IFN-γ+	2,29 ± 0,50 %	3,97 ± 0,93 %	0.13	1,75 ± 0,19 %	1,83 ± 0,42 %	0.45
CD4+ IL-17+	4,59 ± 1,84 %	2,95 ± 0,10 %	0.23	ND	ND	ND
Splenocytes						
CD4+ IFN-γ+	2,63 ± 1,24 %	3,86 ± 1,21 %	0.28	1,00 ± 0,15 %	1,08 ± 0,09 %	0.32
CD4+ IL17+	2,17 ± 0,36 %	1,44 ± 0,05 %	0.11	ND	ND	ND
CNS-infiltrating cells						
CD4+ IFN-γ+	9.08 ± 1,09 %	16.75 ± 2,09 %	**0.002**	2,46 ± 0,40 %	3,75 ± 0,53 %	**0.02**
CD4+ IL17+	6,7 ± 1,02 %	7,79 ± 1,79 %	0.18	ND	ND	ND
CD25+ FoxP3+	3.06 ± 0.83 %	2.50 ± 0.77 %	0.31	ND	ND	ND

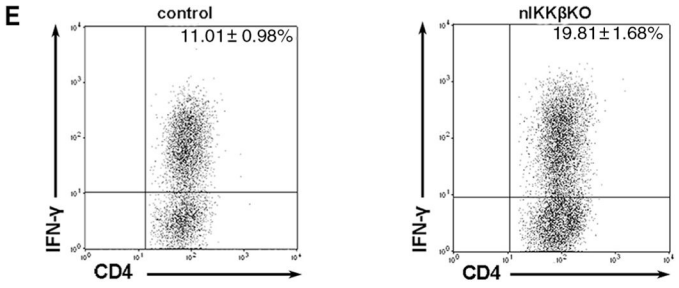

FIGURE 6.

nIKK*β*KO mice show normal T cell priming, enrichment of $CD4^+$ and $CD4^+IFN\text{-}\gamma^+$ T cells and reduction in $NK1.1^+$ cells in the spinal cord at the peak and chronic phase of EAE. *A* and *B*, Draining LN cells and splenocytes were isolated from nIKK*β*KO and control mice 9 days after immunization with $MOG_{35–55}$ peptide and restimulated with $MOG_{35–55}$ peptide for 72 h. No differences in cell proliferation of LN cells (*A*) and splenocytes (*B*) were detected between MOG-specific T cells from nIKK*β*KO and control mice. Cell proliferation results are expressed as the stimulation index (ratio between radioactivity counts of cells cultured in the presence of $MOG_{35–55}$ peptide and cells cultured with medium alone). *C*,

CNS-infiltrating monocytes from spinal cords were isolated at the peak and chronic phase of disease from control and nIKKβKO mice. Cells were stained for the surface markers CD4, CD8, B220, NK1.1, and CD11b. Three independent samples from one representative experiment were analyzed for each condition and the percentages of the surface marker-expressing cells ± SEM in the total live cell gates are indicated in the table. *D* and *E*, Draining LN cells, splenocytes, and CNS-infiltrating monocytes from spinal cords were isolated at the peak and chronic phase of disease from control and nIKKβKO mice. Cells were stimulated with PMA/ionomycin and stained for the surface markers CD4 and CD25 and by intracellular staining for the cytokines IFN-γ, IL-17, and transcription factor FoxP3. Three independent samples from each of two different experiments were analyzed for each condition and the percentages of the cytokine-secreting cells ± SEM in the total live cell gates are indicated in the table (*D*). On the dot plots (*E*), the analysis for the CNS-infiltrating cells of a representative experiment (day 17) is presented. The plots show the $CD4^+$CNS-derived T cells in the total live-cell gate. ND, Not done.

Table I

Incidence, clinical severity, and mortality rate of $MOG_{35–55}$-induced EAE in nIKKβKO and control mice[a]

Mice	Incidence	Mean Day of Onset	Mean Maximal Score	Cumulative Score (days of EAE follow-up)	Mortality Rate
Expt. 1					
C57BL/6 WT	5/5 (100%)	8 ± 0.00	3 ± 0.35	98.9 (128)	0/5 (0%)
nIKKβKO	5/5 (100%)	8.2 ± 0.15	3.5 ± 0.15	129.1 (128)	0/5 (0%)
Expt. 2					
IKK$\beta^{F/F}$ control	8/8 (100%)	8.8 ± 0.8	3 ± 0.35	85.87 (123)	1/8 (12.5%)
nIKKβKO	8/8 (100%)	8.75 ± 0.62	3.27 ± 0.18	110.7 (123)	2/8 (25%)
Expt. 3					
IKK$\beta^{F/F}$ control	20/20 (100%)	10.3 ± 0.25	3.19 ± 0.11	59.76 (43)	0/20 (0%)
nIKKβKO	20/20 (100%)	10.9 ± 0.41	3.35 ± 0.07	83.18 (43)	6/20 (30%)

[a]The data presented are from three independent experiments. $MOG_{35–55}$-EAE in IKK$\beta^{F/F}$ control mice shows an identical clinical profile as in C57BL/6 WT mice. Mean day of onset is expressed as day after immunization ± SEM and mean maximal score is presented as mean maximal score ± SEM. Cumulative score is calculated by summing up each individual score registered during the follow-up period.